Journal of Science and Technology in Civil Engineering, NUCE 2021. 15 (1): 41–54

THE INFLUENCE OF SATURATION ON THE INTERFACE SHEAR STRENGTH OF CLAY AND NONWOVEN GEOTEXTILE

Minh-Duc Nguyen[a,*], Minh-Phu Ho[a]

[a]*Faculty of Civil Engineering, Ho Chi Minh City University of Technology and Education, 01 Vo Van Ngan street, Thu Duc district, Ho Chi Minh city, Vietnam*

Article history:
Received 09/10/2020, Revised 24/11/2020, Accepted 04/12/2020

Abstract

The paper presents a series of modified direct shear tests to investigate the interface shear strength between clay and nonwoven geotextile under different normal stresses and degrees of saturation. The modified direct shear apparatus consists of a 60 mm × 60 mm square shear box assembly with a 60 mm × 60 mm acrylic block inserted in the bottom shear box. A woven geotextile layer was glued to the top of the acrylic block, while the top shear box was filled by the compacted clayey soil. The results revealed that the interface shear strength of clay and nonwoven geotextile reduced by 13.4-27.7% when changing from optimum moisture content (OMC) of the soil to saturation condition. The high permeability of nonwoven geotextile induced the dissipation of excess pore water pressure at the interface when shearing. As a result, the adhesion factor of the clay-geotextile interface increased from about 0.6 for the specimens at OMC to over 0.8 for consolidated saturated specimens. In contrast, for the impermeable reinforcement, the interface shear strength analysis of previous studies shows that the adhesion factor of the reinforcement and clayey soil would be reduced when increasing the water content of the clay specimens.

Keywords: adhesion factor; clay; nonwoven geotextile, interface shear strength; saturation.

https://doi.org/10.31814/stce.nuce2021-15(1)-04

1. Introduction

Recently, geosynthetics reinforced soil (GRS) structure was widely used in the interest of several distinct advantages over the conventional retaining structures. Most of the current design guidelines for GRS structures specify using the high permeable materials (such as sandy soil) as backfill materials within reinforced soil and preclude the use of clayey soil [1–4]. In Mekong Delta, most of the sandy soil was excavated from riverbeds, of which the resource has been reduced over the years. As a result, the sand is expensive and induced the high cost of GRS structures.

To reduce the construction cost and minimize the transportation cost and environmentally impacted associated with the riverbed sandy soil excavation, locally available clayey soil has been used as the alternative backfills. The main concern with using clay as backfill is the rise of pore water pressure in the low permeable soil and weaken the soil strength after rainfalls. Especially, for the mud generated from dredging work using hydraulic pumping method, the low permeability characteristic

*Corresponding author. *E-mail address:* ducnm@hcmute.edu.vn (Nguyen, M.-D.)

of the soil induces a long period to solidify, which might cause severe environmental and ecological issues in its surrounding area [5]. However, several previous studies illustrated that those problems could be appropriately alleviated by adopting suitable construction techniques and drainage systems [6, 7].

The permeable geosynthetics exhibited the potential of improving the shear strength of clayey soils. Under consolidated undrained triaxial compression, the permeable geosynthetics layer induced the increment in both shear strength and excess pore water pressure in the reinforced clay due to the lateral restraint of reinforcement layers [8, 9].

Besides, several studies focused on investigating the interface shear strength of soil and geosynthetics under both unsaturated [10–13] and saturated conditions [11, 14]. The interface friction angle between compacted clay liner and smooth geomembrane was about 6.5-10.50 for both dry and wet conditions [15]. For bentonite, the increment in the water content of the bentonite specimens induced reducing in the interface friction angle but increasing in adhesion of the two materials [16]. Similarly, the interface shear strength of clay with different plasticity index and some types of geotextile and geogrid also significantly reduced when increasing the water content of the soil [17].

The interface shear behaviors of saturated clay specimens under the undrained condition have been investigated previously. The undrained shearing condition was suggested when the shearing rate reached 0.9-2mm/min [10, 12, 16]. The adhesion factor is defined as the ratio of the interface shear strength and the shear strength of the soil under the same soil density, water content, and normal stress condition. Due to the higher permeability and transmissivity, the adhesion factor of clay-nonwoven fabric could be higher than that of clay-woven fabric under the undrained direct shear test [10]. The investigation of clay-geosynthetics interface behavior revealed that the reinforcement efficiency (i.e., adhesion factor) of cohesive soils was markedly affected by the molding moisture contents. The increase in molding moisture content can significantly reduce the reinforcement efficiency due to the reduction of the soils' suction with the increase in moisture content and the possible development of excess pore water pressure in relatively saturated clays, which reduces the effective stresses and the shear resistance [17]. The same interface shear behavior was observed in Polyethylene geosynthetics–clay interface under near-undrained shearing condition [16]. Nevertheless, the variation of the adhesion factor of nonwoven geotextile and clay when changing from OMC to the undrained saturation condition has been rarely reported in the previous studies.

Based on the above discussions, the paper proposed the investigation of interface shear strength behavior of clay and nonwoven geotextile under both OMC and saturated conditions. The specimens were compacted, saturated, and consolidated before shearing using a modified 60 × 60 mm square shear box. The shearing rate was set at 1 mm/min, in which the undrained condition could be relatively achieved. The experimental results would illustrate the influence of the saturation process on the interface shear strength behavior of clay and nonwoven geotextile. The study also analyzed the role of permeable geosynthetics on improving the adhesion factor of clay and reinforcements under the undrained condition.

2. Experimental program

2.1. Clay

Clayey soil was excavated from Cai Lon river, Kien Giang province. It is classified as high plasticity inorganic clay (MH) by the Unified Soil Classification System with a specific gravity (Gs) of

2.75. The liquid limit (LL), plastic limit (PL), and plasticity index (PI) are 91.5, 44.9, and 46.6, respectively. The standard proctor compaction test [17] shows that the optimum moisture content and maximum dry unit weight are 24.5% and 15.02 kN/m^3, respectively (Fig. 1).

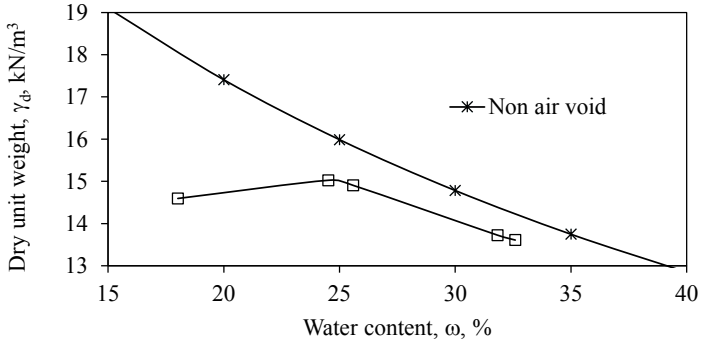

Figure 1. Proctor compaction test of the clay using standard compaction energy

2.2. Geotextile

A commercially available polyethylene terephthalate nonwoven geotextile was used. The tensile test results indicate that the geotextile is an anisotropic tensile material, in which the tensile strength in the longitudinal direction (i.e., stronger direction) was higher than that in the transverse direction (Table 1). The geotextile is high permeability material with cross-plane permeability, $k = 3.6 \times 10^{-3}$ m/sec.

Table 1. Properties of the nonwoven geotextile

Properties	Value
Mass (g/m^2)	200
Thickness, (mm)	1.45
Longitudinal ultimate tensile strength (kN/m)	9.28
Transverse ultimate tensile strength (kN/m)	7.08
Longitudinal tensile strain at failure, (%)	84.1
Transverse tensile strain at failure, (%)	117.8
Cross-plane permeability, k (m/sec)	3.6×10^{-3}

2.3. Specimen preparation

The soft clay was dried was placed in an oven at 600 °C for a minimum of 24h and then crushed and grounded into dry powder in a mortar. The dry soil was then mixed with an amount of water corresponding to the optimum moisture content, OMC = 24.5%. It was placed in a resealable plastic bag within a temperature-controlled chamber, and sealed for a minimum of 2 days to ensure a uniform distribution of moisture within the soil mass. The soil preparation for the test was similar to that for the standard compaction test suggested by ASTM D698 [18].

A series of direct shear tests and interface direct shear tests were performed on unreinforced clay under OMC (i.e., dry condition) and saturation (i.e., wet condition) using 60 mm × 60 mm × 20 mm

(i.e., width, length, and thickness, respectively) shear box (Fig. 2(a)). In order to prepare unreinforced specimens, the clay was compacted in the shear box using a tamper to reach the target dry unit weight $\gamma_{d-\max} = 15.02$ kN/m^3.

The interface shear behavior was determined using the modified shear box, of which an acrylic block filled the lower shear box with a geotextile layer glue on the top (Fig. 2(b)). The layer was also fixed to the lower shear box by screws, of which the longitudinal direction was placed along the shear direction. Its length was longer than the length of the upper shear box by 1 cm to avoid the changes in the interface shear area when shearing (Fig. 2(c)). The soil conditions were prepared similarly to that of unreinforced clay, in which the dry unit weight was 15.02 kN/m^3 at either OMC or saturation condition. The presented testing method was similar to that proposed in previous studies [11, 12, 14].

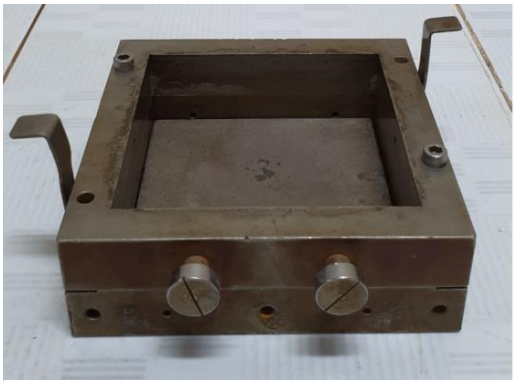

(a) 60 mm × 60 mm square shear box

(b) Bottom shear box filled by acrylic block

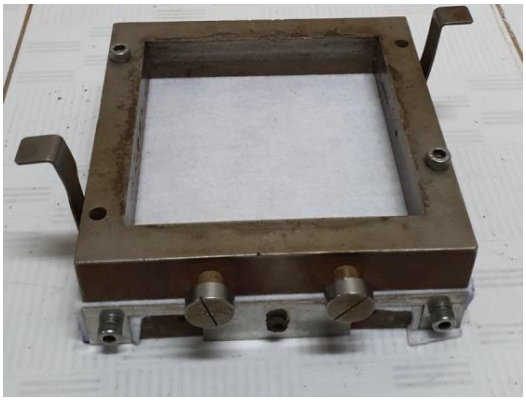

(c) Geotextile layer fixed on the bottom shear box

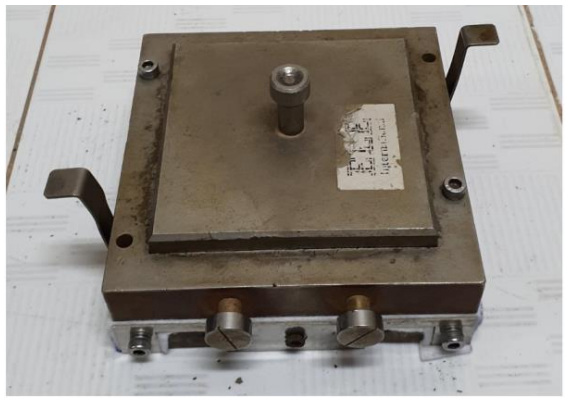

(d) Complete specimen preparation for interface shear test

Figure 2. Photos of the shear box

It should be noted that the dimension of the proposed shear box (i.e., 60 mm × 60 mm) was smaller than that recommended determining the interface shear strength by direct shear, in which the sides of the square or rectangular shear device should be at least 300 mm [19]. The smaller size of the shear box can result in a higher shear strength than from a 300 mm shear box in peak condition while giving nearly the same residual strength [20–23]. Nevertheless, the smaller shear boxes (i.e., 60 mm × 60 mm) have been used to obtain valuable information on interface behavior [14, 24, 25]. Therefore, it was assumed in the current study that any increases in soil strength due to the smaller

shear area were the same for all specimens under the same normal stress and water content condition. The adhesion ratio herein thus would be a little higher than that obtained using a bigger shear box.

2.4. Test procedure

A total of 8 direct shear tests and eight interface direct shear tests were performed for both unsaturated and saturated specimens under four normal stresses, 50 kPa, 100 kPa, 200 kPa and 400 kPa. For unsaturated specimens, the shear test was performed after preparing the compacted specimens. For saturated specimens, they were soaked in de-air water for 24h, applied normal stress for another 24h to complete the consolidation process. Both saturation and consolidation process of specimens were adopted to ASTM D5321 [19]. For both direct shear tests and interface shear tests, the shear rate was set at 1 mm/min to ensure the close-undrained condition, which was also adopted in previous studies [10, 12]. The test was ended when the shear displacement reached 13 mm, which was the limitation of the testing apparatus. The repeatability and consistency of the test results were examined by conducting a few tests on the specimens under the same conditions.

3. Results

3.1. Shear strength behavior of clay

Fig. 3 presents the shear strength behaviors of clay under different normal stress and water content. For the clay at its optimum moisture content, its peak shear strength reached when the shear

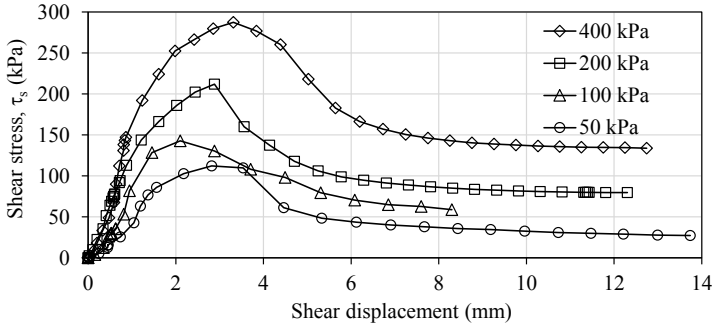

(a) At optimum moisture content

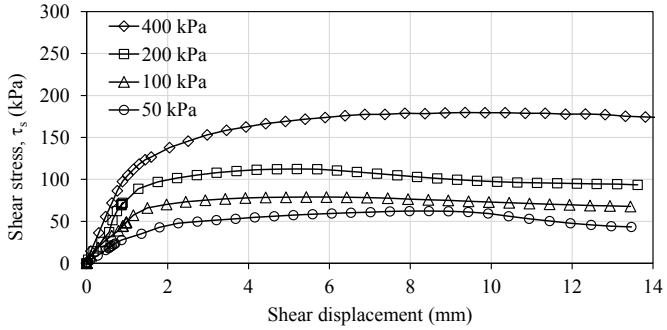

(b) After consolidation in the saturated condition

Figure 3. Shear strength behavior of compacted clay under different normal stresses

displacement was about 2-3 mm (Fig. 3(a)). The higher the normal stress, the higher the shear stress was obtained. On the other hand, after fully consolidated in the saturated condition, the shear strength of the clay was reduced, and the shear displacement at failure was much higher (i.e., over 6 mm) than that of clay at its OMC. The similar shear behaviors of clay were also observed when changing water content of the soil [26].

The failure envelopes of the compacted clay under OMC and consolidation in the saturated condition were shown in Fig. 4. Compared to the shear strength of clay at OMC, both friction angle and cohesion of the compacted clay after consolidated were reduced significantly. In particular, the friction angle and cohesion were reduced from 27.80 to 4.70 and 96.0 kPa to 62.6 kPa, respectively (Table 2). After saturation, the clay specimens exhibited the near-undrained shear strength (i.e., very low friction angle) under 1 mm/min of shearing rate. The shear strength reduction of the compacted clay was caused by the loss of suction of the soils with the increase in moisture content and the possible development of excess pore water pressure in saturated clays, which reduces the effective stresses and the shear resistance [16].

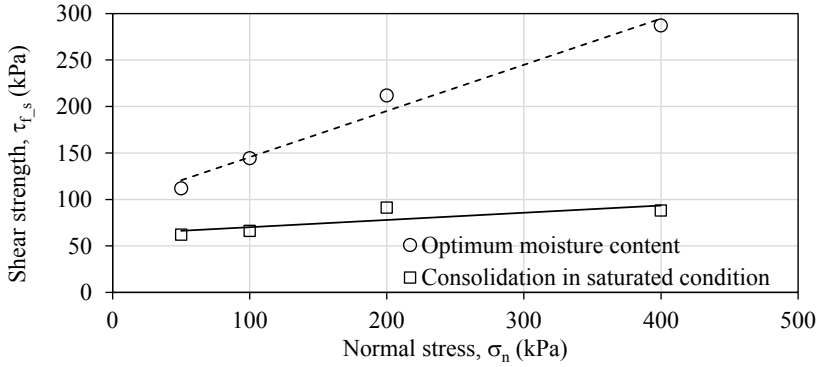

Figure 4. Failure envelope of shear strength behavior of compacted clay

Table 2. Shear strength and interface shear strength results of the compacted clay and the clay-geotextile interface

Water content	Materials	Cohesion (kPa)	Friction angle (degree)
OMC	Clay	96.0	27.8
	Clay-geotextile interface	41.9	23.1
Consolidation in the saturated condition	Clay	62.6	4.7
	Clay-geotextile interface	24.0	21.5

3.2. Interface shear strength behavior of clay and nonwoven geotextile

Fig. 5 presents the interface shear strength behavior of clay and nonwoven geotextile. At optimum moisture content, the hardening stress-deformation behavior was observed in the interface shear strength behavior of the clay and geotextile, in which no definite peak was noticed on the stress-deformation curve (Fig. 5(a)). Therefore, 12.7 mm of shear displacement was considered the deformation at failure [19].

On the other hand, when the clay and geotextile specimens were consolidated in the saturated condition, the shear stress-deformation behavior was more brittle. The peak interface shear strength

was observed when the shear displacement was about 3-6 mm (Fig. 5(b)). The brittle interface shear failure of saturated clay and geotextile was also reported in previous studies, which might be due to the penetration of clay particles into the nonwoven geotextile layer during the consolidation process [11–13].

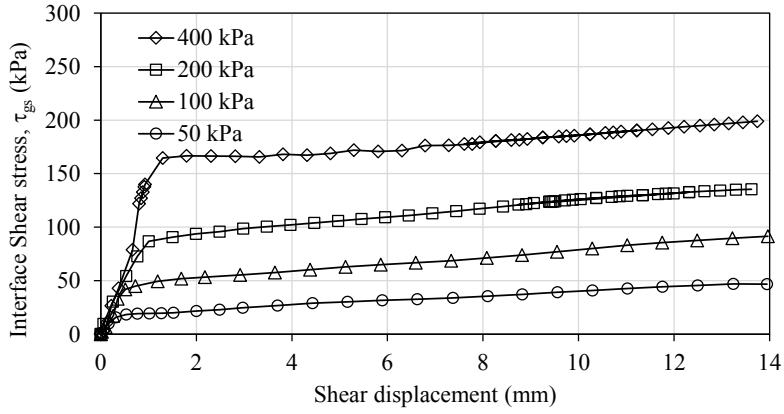

(a) At optimum moisture content

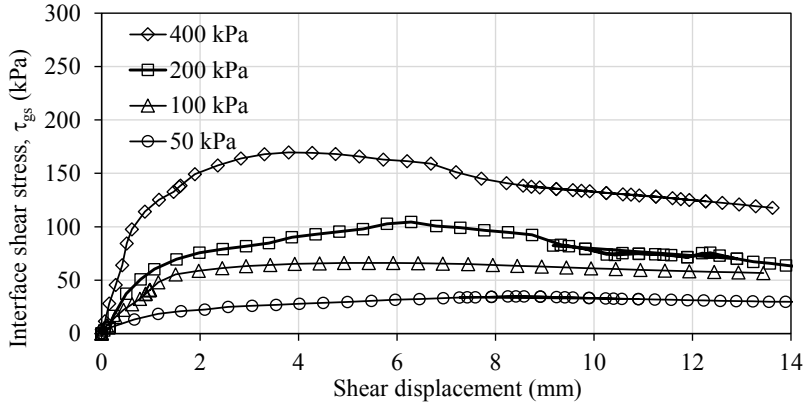

(b) After consolidation in the saturated condition

Figure 5. Interface shear strength behavior under different normal stresses

Fig. 6 shows the failure envelopes of interface shear strength of compacted clay and geotextile, in which the interface shear strength was chosen as the shear stress at 12.7 mm of shear displacement and the peak value for the clay specimens at optimum moisture content and consolidation in the saturated condition, respectively. Similar to the shear strength of compacted clay, the interface shear strength reduced significantly due to the consolidated process in saturation condition. However, unlike the shear strength behavior of compacted clay, while the interface cohesion was reduced remarkably from 41.9 kPa to 24.0 kPa, the interface friction angle was only slightly decreased after the consolidation process (Table 2).

Besides, the shear strength of the compacted clay was higher than the interface shear strength of the clay-geotextile at both optimum moisture content and consolidation in the saturated condition. This behavior was in agreement with the results reported in the previous studies [14, 16].

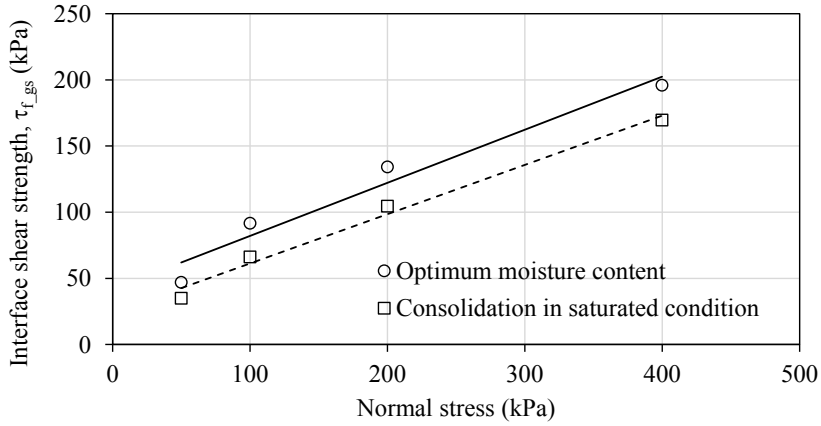

Figure 6. Failure envelop of interface shear strength of clay-geotextile

3.3. Interface shear strength reduction due to saturation

As mentioned previously, the consolidation process in the saturated condition significantly reduced the shear strength of the clay and the clay-geotextile interface. In order to quantify the loss of shear strength and interface shear strength after saturation, the reduction in shear strength and interface shear strength were evaluated for the clay and the clay-geotextile interface, respectively. For the unreinforced clay specimens, the shear strength reduction was evaluated as:

$$\Delta\tau_{f\_s} = \tau_{f\_s}^{OMC} - \tau_{f\_s}^{sat} \tag{1}$$

in which $\tau_{f\_s}^{OMC}$ and $\tau_{f\_s}^{sat}$ are the shear strength of the clay specimens at OMC and consolidation in the saturated condition, respectively.

Similarly, the interface shear strength reduction $\Delta\tau_{f\_gs}$ was the difference of the clay-geotextile interface shear strength at OMC, $\tau_{f\_gs}^{OMC}$ and that after consolidation in the saturated condition $\tau_{f\_gs}^{sat}$.

$$\Delta\tau_{f\_gs} = \tau_{f\_gs}^{OMC} - \tau_{f\_gs}^{sat} \tag{2}$$

In addition, the shear strength reductions of the clay and the clay-geotextile interface were also calculated in percentage. The percent shear strength reduction of the clay $\%\Delta\tau_{f\_s}$ was evaluated as:

$$\%\Delta\tau_{f\_s} = \left(1 - \frac{\tau_{f\_s}^{sat}}{\tau_{f\_s}^{OMC}}\right) \times 100\% \tag{3}$$

The percent interface shear strength reduction $\%\Delta\tau_{f\_gs}$ would be estimated for the clay-geotextile interface, accordingly:

$$\%\Delta\tau_{f\_gs} = \left(1 - \frac{\tau_{f\_gs}^{sat}}{\tau_{f\_gs}^{OMC}}\right) \times 100\% \tag{4}$$

Fig. 7 illustrates the variation of the shear strength reduction $\Delta\tau_{f\_s}$ and the interface shear strength reduction $\Delta\tau_{f\_gs}$ with normal stress. The results show that the $\Delta\tau_{f\_s}$ of the compacted clay due to saturation was about 50-108 kPa. The higher the normal stress, the higher the shear strength reduction would be. However, the value of $\Delta\tau_{f\_gs}$ was only about 12-30 kPa, which was less than one fourth to

one third of the value of $\Delta\tau_{f\_s}$ under the same normal stress (Table 3). It was apparently due to the high permeability and transmitivity of the nonwoven geotextile. After saturation, the interface shear would induce the development of excess porewater pressure, which would be dissipated to the high permeable nonwoven geotextile layer. This phenomenon would improve the interface clay-geotextile shear strength. In other words, the nonwoven geotextile was minimized the interface shear strength reduction due to the saturation process of clay specimens.

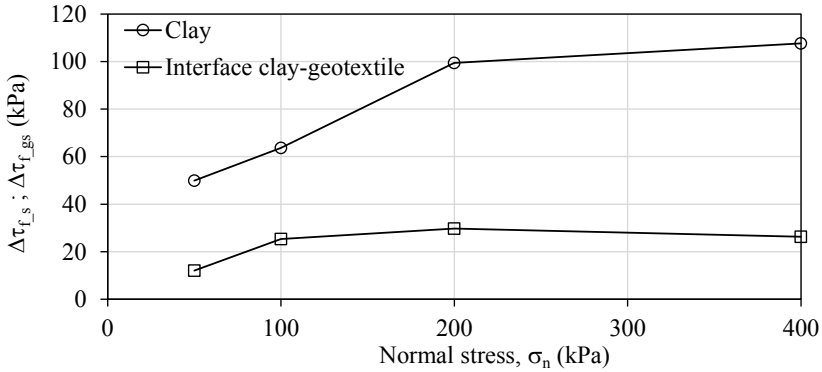

Figure 7. The reduction in shear strength of the clay and interface shear strength of the clay-geotextile interface due to saturation

Table 3. Shear strength difference and percent shear strength reduction of the clay and clay-geotextile interface due to saturation

Normal stress, σ_n (kPa)	$\Delta\tau_{f\_s}$ (kPa)	$\%\Delta\tau_{f\_s}$ (%)	$\Delta\tau_{f\_gs}$ (kPa)	$\%\Delta\tau_{f\_gs}$ (%)
50	50	44.5	12	25.7
100	64	44.6	25	27.7
200	99	46.9	30	22.2
400	108	37.5	26	13.4

The influence of normal stress in the shear strength behaviors of clay and the interface shear strength of the clay-geotextile interface was different. As shown in Fig. 4, the shear strength of clay at OMC increased significantly with normal stress increment. Meanwhile, the shear strength of saturated clay increased marginally when the normal stress raised from 50 kPa to 400 kPa. As a result, the shear strength reduction of clay after saturation $\Delta\tau_{f\_s}$ was increased consistently with the normal stress increment (Fig. 7). It was suggested that the more shear strength loss of clay due to saturation would be observed, especially under high normal stress.

On the other hand, the reduction in the interface shear strength of the clay-geotextile interface was increased for the lower normal stress (i.e., σ_n = 50-100 kPa) and changed marginally for the higher normal stress (i.e., σ_n = 100-400 kPa). For lower normal stress σ_n = 50 kPa, the geotextile-saturated clay interaction was practically drained (friction-like [10]), which induced the high interface shear strength and low interface shear strength reduction after saturated. Under the higher normal stress, the excess porewater pressure would develop in the saturated clay, which decreased the interface shear strength and increased the interface shear strength reduction. As explained previously, the excess porewater pressure would be able to dissipate through the high permeability and transmitivity

geotextile layer, which induced the partly drained behavior of geotextile – saturated clay interaction [10]. That explained the observation of slight changes in the interface friction angle of geotextile-clay when changing from OMC to saturated condition. As shown in Fig. 6, the failure envelopes of interface shear strength of clay-geotextile at OMC and at saturation were approximately parallel for a range of normal stress from 100 kPa to 400 kPa. Thus, changes of σ_n did not induce any significant changes in the interface shear strength reduction $\Delta\tau_{f\_gs}$ (Table 3).

The percent reduction of the shear strength and the interface shear strength of specimens under different normal stress were given in Table 3. The results revealed that the interface shear strength of clay-geotextile decreased by 13.4-27.7% after completed consolidation in the saturated condition, whereas the shear strength reduction of the compacted clay due to saturation was much higher, about 37.5- 46.9%. The high percent shear strength reduction due to saturation of clay was also reported in previous studies. The wetting effect would reduce the friction and the cohesion among soil particles resulting in the shear strength reduction [27, 28].

3.4. Adhesion factor of the interface of clay and nonwoven geotextile

The adhesion factor, also known as contact efficiency, is the factor that exhibited the soil-reinforcement interaction [10]. It is a fundamental factor to design the geosynthetics reinforced soil structures [29–31]. The adhesion factor was the ratio of the interface shear strength over the soil's shear strength under the same normal stress and soil condition.

$$R_f = \frac{\tau_{f\_gs}}{\tau_{f\_s}} \tag{5}$$

Fig. 8 illustrates the adhesion factor results of the clay-geotextile interface at OMC and after consolidated in the saturated condition. In general, the clay-geotextile adhesion factor increased with the increment of normal stress. For the clay specimens at OMC under σ_n = 50 kPa, the value of R_f was relatively small, R_f = 0.42. Under the higher normal stress σ_n = 100-400 kPa, the adhesion factor was as high as 0.63-0.68. The obtained results agreed with the range value of the adhesion factor of clay and nonwoven geotextile R_f = 0.64-0.78 reported previously [17]. The slight difference in R_f might be due to the difference in materials (i.e., soil and geosynthetics) and the size of the shearing box. After consolidating in the saturated condition, the clay-geotextile adhesion factor was higher, R_f = 0.83-0.94 under 100-400 kPa of normal stress (Fig. 8). Those results were contrasted to the shear strength reduction of the clay-geotextile interface due to saturation discussed previously. In the clay after compaction at OMC with the degree of saturation S_r = 84.6%, the negative porewater pressure appeared and created the suction in the unsaturated clay. The higher suction, the higher shear strength was obtained. When applying the normal stress, the excess porewater pressure would not occur in the soil with S_r < 90% [32, 33], the suction would maintain in the unsaturated clay, which induced the high shear strength of clay at OMC. Compared to the unsaturated clay-geotextile interface, the suction caused by the negative porewater pressure might diminish at the interface due to the high permeability of nonwoven geotextile, which decreased the interface shear strength. Thus, the adhesion factor (i.e., the ratio of τ_{f_gs} and τ_{f_s}) was small.

In contrast, under normal stress, the excess pore water pressure developing in the saturated clay specimens and reduced the shear strength. During the shearing process between the saturated clay and geotextile interface, the excess porewater pressure would be dissipated to the high permeability geotextile layer, which maintained the high interface shear strength. As a result, the adhesion factor of clay-geotextile specimens at the saturated condition could be higher than that at the OMC condition.

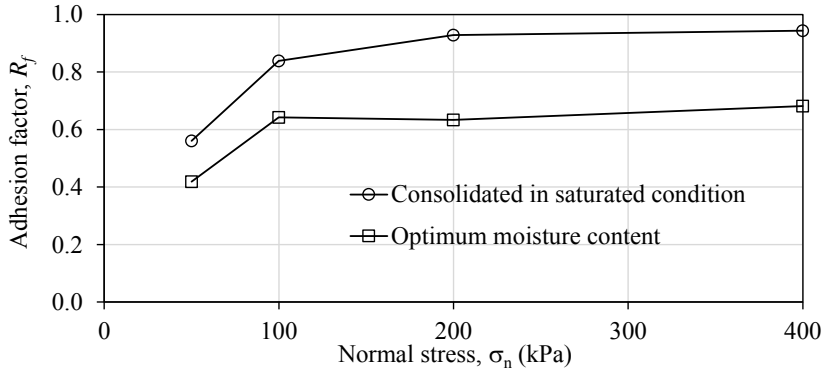

Figure 8. The adhesion factor of clay-geotextile under different normal stresses

The observation was in agreement with the obtained results after reanalyzing the previous experimental results of the clay-geotextile interface. The clay specimens with the plasticity index, PI = 25 was compacted at different water content and examinated to evaluate the interface shear strength with geotextile and polypropylene geogrid [17]. As shown in Fig. 9(a), when increasing the water content of the clay from 11% to 20%, the adhesion factor of the clay-geotextile was also increased from less than 0.67 to over 0.73 for the ranger of normal stress from 25 kPa to 75 kPa. However, the contradicted behavior of the adhesion factor was found in that clay and polypropylene geogrid interface. The increment of water content induced a decrease in the value of R_f, which was independent on the value of normal stress (Fig. 9(b)). The porewater pressure measurement at the unsaturated clay - HDPE geomembrane interface showed that the negative porewater pressure and suction were found and maintained at the interface due to the impermeable HDPE geomembrane [11]. When increasing the water content, the clay was about to saturate. Like the HDPE geomembrane, polypropylene geogrid was a low-permeable material, unable to dissipate the excess porewater pressure developing in the clay - polypropylene geogrid interface during shearing. The higher excess in porewater pressure

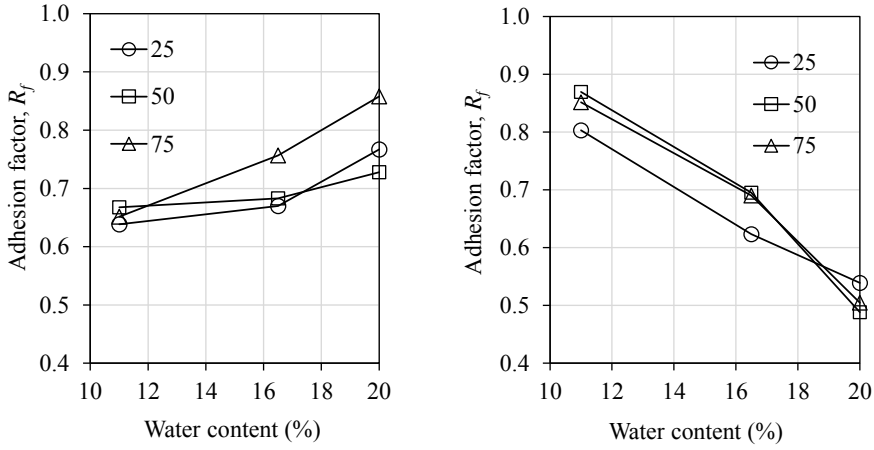

Figure 9. The variation of adhesion factor, R_f with water content under 25 kPa, 50 kPa, and 75 kPa of normal stress (reanalyzed from experimental results [17])

caused the lower interface shear strength. Thus, the adhesion factor of the clay and low permeability geosynthetics would be decreased when increasing the water content of the clay specimens. A similar observation was reported in the sand-bentonite mixture and geomembrane interface, in which the adhesion factor was smaller for the higher water content specimens [11]. The adhesion factor analysis illustrates the advantages of permeable geosynthetics on improving the saturated clay-reinforcement interaction.

4. Conclusions

In this study, a series of modified interface direct shear test was performed to investigate the interface shear strength behavior of clay-nonwoven geotextile under different normal stresses and degrees of saturation. The shearing rate was set at 1 mm/min to develop the near-undrained condition during tests. The obtained results illustrated the advantages of high permeable nonwoven geotextile on maintaining the high adhesion factor at OMC and after saturation. The following conclusions were drawn from this study.

- When changing from OMC to consolidation in a saturated condition, both friction angle and cohesion of the compacted clay were significantly reduced. The percent reduction in shear strength of the compacted clay due to saturation was 37.5-46.9%. The failure pattern of the clay specimens was transferred from brittle failure at OMC to more ductile failure at saturation.

- The interface shear strength reduction due to saturation was about 13.4-27.7%. In particular, there was a slight decrement in interface friction angle (about 1.60) while the interface cohesion remarkably reduced from 41.9 kPa to 24.0 kPa.

- Under 100-400 kPa of normal stress, the adhesion factor of clay-geotextile at OMC was about 0.64-0.68. This factor increased to 0.83-0.94 after consolidation in a saturated condition. This increment would be due to the high permeability of geotextile, which dissipated the excessive porewater pressure in the clay-geotextile interface when shearing. For the impermeable geosynthetics-clay interface behavior, the increment of the water content of the clay caused the decrement in the adhesion factor.

This study promoted high permeability nonwoven geotextile advantages on maintaining high clay-reinforcement interface shear strength after saturation.

Acknowledgments

The authors gratefully acknowledge the support and advice of graduate students and lecturers in Ho Chi Minh City University of Technology and Education. The comments and suggestions by anonymous reviewers are greatly appreciated.

References

[1] Elias, V., Christopher, B. R., Berg, R. (2001). *Mechanically Stabilized Earth Walls and Reinforced Soil Slopes Design and Construction Guidelines*. Report No. FHWA-NHI-00-043. National Highway Institute, Federal Highway Administration, Washington, D.C.

[2] AASHTO (2002). *Standard Specifications for Highway Bridges*. 17th edition, Washington, D.C., American Association of State Highway and Transportation Officials.

[3] Berg, R., Christopher, B. R., Samtani, N. (2009). *Design of Mechanically Stabilized Earth Walls and Reinforced Soil Slopes*. Vol. I and II, Report No. FHWA-NHI-10-024, National Highway Institute, Federal Highway Administration, Washington, D.C.

[4] NCMA. *Design manual for segmental retaining walls*. Herndon, VA, National Concrete Masonry Association.
[5] Dong, P. H. (2018). Influence of vertical drains on improving dredged mud by vacuum consolidation method. *Journal of Science and Technology in Civil Engineering (STCE)-NUCE*, 12(5):63–72.
[6] Zornberg, J. G., Mitchell, J. K. (1994). Reinforced soil structures with poorly draining backfills. Part I: Reinforcement interactions and functions. *Geosynthetics International*, 1(2):103–147.
[7] Mitchell, J. K., Zornberg, J. G. (1995). Reinforced soil structures with poorly draining backfills part II: case histories and applications. *Geosynthetics International*, 2(1):265–307.
[8] Ingold, T. S., Miller, K. S. (1982). The performance of impermeable and permeable reinforcement in clay subject to undrained loading. *Quarterly Journal of Engineering Geology and Hydrogeology*, 15(3): 201–208.
[9] Yang, K.-H., Nguyen, M. D., Yalew, W. M., Liu, C.-N., Gupta, R. (2016). Behavior of Geotextile-Reinforced Clay in Consolidated-Undrained Tests: Reinterpretation of Porewater Pressure Parameters. *Journal of GeoEngineering*, 11(2):45–57.
[10] Fourie, A. B., Fabian, K. J. (1987). Laboratory determination of clay-geotextile interaction. *Geotextiles and Geomembranes*, 6(4):275–294.
[11] Fleming, I. R., Sharma, J. S., Jogi, M. B. (2006). Shear strength of geomembrane–soil interface under unsaturated conditions. *Geotextiles and Geomembranes*, 24(5):274–284.
[12] Fishman, K. L., Pal, S. (1994). Further study of geomembrane/cohesive soil interface shear behavior. *Geotextiles and Geomembranes*, 13(9):571–590.
[13] Fox, P. J., Rowland, M. G., Scheithe, J. R. (1998). Internal shear strength of three geosynthetic clay liners. *Journal of Geotechnical and Geoenvironmental Engineering*, 124(10):933–944.
[14] Jotisankasa, A., Rurgchaisri, N. (2018). Shear strength of interfaces between unsaturated soils and composite geotextile with polyester yarn reinforcement. *Geotextiles and Geomembranes*, 46(3):338–353.
[15] Bergado, D. T., Ramana, G. V., Sia, H. I., Varun (2006). Evaluation of interface shear strength of composite liner system and stability analysis for a landfill lining system in Thailand. *Geotextiles and Geomembranes*, 24(6):371–393.
[16] Chai, J.-C., Saito, A. (2016). Interface shear strengths between geosynthetics and clayey soils. *International Journal of Geosynthetics and Ground Engineering*, 2(3):19.
[17] Abu-Farsakh, M., Coronel, J., Tao, M. (2007). Effect of soil moisture content and dry density on cohesive soil–geosynthetic interactions using large direct shear tests. *Journal of Materials in Civil Engineering*, 19 (7):540–549.
[18] ASTM D698. *Standard test methods for laboratory compaction characteristics*. West Conshohocken, PA: ASTM International.
[19] ASTM D5321. *Standard Test Method for Determining the Shear Strength of Soil-geosynthetic and Geosynthetic-geosynthetic Interfaces by Direct Shear*. West Conshohocken, PA: ASTM International.
[20] Palmeira, E., Milligan, G. W. E. (1989). Scale effects in direct shear tests on sand. In *Proceedings of the XII International Conference on Soil Mechanics and Foundation Engineering*, volume 1, Rio de Janeiro, Brazil, 739–742.
[21] Cerato, A. B., Lutenegger, A. J. (2006). Specimen size and scale effects of direct shear box tests of sands. *Geotechnical Testing Journal*, 29(6):507–516.
[22] Wu, P.-K., Matsushima, K., Tatsuoka, F. (2008). Effects of specimen size and some other factors on the strength and deformation of granular soil in direct shear tests. *Geotechnical Testing Journal*, 31(1):45–64.
[23] Ziaie Moayed, R., Alibolandi, M., Alizadeh, A. (2017). Specimen size effects on direct shear test of silty sands. *International Journal of Geotechnical Engineering*, 11(2):198–205.
[24] Khoury, C. N., Miller, G. A., Hatami, K. (2011). Unsaturated soil–geotextile interface behavior. *Geotextiles and Geomembranes*, 29(1):17–28.
[25] Basudhar, P. et al. (2010). Modeling of soil–woven geotextile interface behavior from direct shear test results. *Geotextiles and Geomembranes*, 28(4):403–408.
[26] Wei, Y., Wu, X., Xia, J., Miller, G. A., Cai, C., Guo, Z., Hassanikhah, A. (2019). The effect of water content on the shear strength characteristics of granitic soils in South China. *Soil and Tillage Research*,

187:50–59.

[27] Abdul Samad, A.R., N. S. J. A. H. M. Z. I. F. R. (2018). Shear Strength Behavior for Unsoaked and Soaked Multistage Triaxial Drained Test. *Advancements in Civil Engineering C & Technology*, 1(4):96–101.

[28] Salman, A. D. (2011). Soaking Effects on the Shear Strength Parameters and Bearing Capacity of Soil. *Engineering and Technology Journal*, 29(6):1107–1123.

[29] Cowell, M. (1993). Comparison of pull-out performance of geogrids and geotextiles. In *Proceedings of Geosynthetics' 93 Conference*, volume 2, 579–592.

[30] Koutsourais, M., Sandri, D., Swan, R. (1998). Soil interaction characteristics of geotextiles and geogrids. In *Proc. 6th Int. Conf. Geosynthetics, Atlanta, Georgia*, 739–744.

[31] Tatlisoz, N., Edil, T. B., Benson, C. H. (1998). Interaction between reinforcing geosynthetics and soil-tire chip mixtures. *Journal of Geotechnical and Geoenvironmental Engineering*, 124(11):1109–1119.

[32] Lins, A. H. P., Sandroni, S. S. (1994). *The development of pore-water presssure in a compacted soil*. CRC Press, Boca Raton, FL, USA.

[33] Nguyen, M.-D., Yang, K.-H., Yalew, W. M. (2020). Compaction behavior of nonwoven geotextile-reinforced clay. *Geosynthetics International*, 27(1):16–33.